Pulsed Production of Antihydrogen in AEgIS

N. Zurlo[1,2,*], *M.* Auzins[3], *B.* Bergmann[4], *G.* Bonomi[2,5], *R.S.* Brusa[6,7], *P.* Burian[4], *A.* Camper[8], *F.* Castelli[9], *R.* Ciury[10], *G.* Consolati[11,12], *M.* Doser[13], *A.* Farricker[14], *L.* Glöggler[13], *Ł.* Graczykowski[15], *M.* Grosbart[13], *F.* Guatieri[7], *N.* Gusakova[13,16], *S.* Haider[13], *S.* Huck[13,17], *M.* Janik[15], *G.* Kasprowicz[15], *G.* Khatri[13], *Ł.* Kłosowski[10], *G.* Kornakov[15], *V.* Krumins[3,13], *L.* Lappo[15], *A.* Linek[10], *J.* Malamant[8,13], *C.* Malbrunot[13], *S.* Mariazzi[6,7], *L.* Nowak[13], *D.* Nowicka[15], *E.* Oswald[13], *D.* Pagano[2,5], *L.* Penasa[6,7], *M.* Piwiński[10], *S.* Pospisil[4], *L.* Povolo[6,7], *F.* Prelz[12], *S.* Rangwala[18], *B.* Rienäcker[13,14], *O.M.* Røhne[8], *A.* Rotondi[2,19], *H.* Sandaker[8], *P.* Smolyanskiy[4], *T.* Sowiński[20], *D.* Tefelski[15], *G.* Testera[21], *M.* Volponi[4,13], *C.P.* Welsch[14], *T.* Wolz[13], *M.* Zawada[10], and *J.* Zielinski[15]
(AEgIS collaboration)

[1]Department of Civil, Environmental, Architectural Engineering and Mathematics, University of Brescia, via Branze 43, 25123 Brescia, Italy
[2]INFN Pavia, via Bassi 6, 27100 Pavia, Italy
[3]University of Latvia, Department of Physics Raina boulevard 19, LV-1586, Riga, Latvia
[4]Institute of Experimental and Applied Physics, Czech Technical University in Prague, Husova 240/5, 11000 Prague 1, Czech Republic
[5]Department of Mechanical and Industrial Engineering, University of Brescia, via Branze 38, 25123 Brescia, Italy
[6]TIFPA/INFN Trento, via Sommarive 14, 38123 Povo, Trento, Italy
[7]Department of Physics, University of Trento, via Sommarive 14, 38123 Povo, Trento, Italy
[8]Department of Physics, University of Oslo, Sem Sælandsvei 24, 0371 Oslo, Norway
[9]Department of Physics, University of Milano, via Celoria 16, 20133 Milano, Italy
[10]Institute of Physics, Faculty of Physics, Astronomy and Informatics, Nicolaus Copernicus University in Toruń, Grudziadzka 5, 87-100 Torun, Poland
[11]Politecnico of Milano, Piazza Leonardo da Vinci 32, 20133 Milano, Italy
[12]INFN Milano, via Celoria 16, 20133, Milano, Italy
[13]Physics Department, CERN, 1211 Geneva 23, Switzerland
[14]University of Liverpool, UK and The Cockcroft Institute, Daresbury, UK
[15]Warsaw University of Technology, Faculty of Physics ul. Koszykowa 75, 00-662, Warsaw, Poland
[16]Department of Physics, NTNU, Norwegian University of Science and Technology, Trondheim, Norway
[17]Department of Physics, University of Hamburg, Jungiusstraße 9, 20355 Hamburg, Germany
[18]Raman Research Institute, C. V. Raman Avenue, Sadashivanagar, Bangalore 560080, India
[19]Department of Physics, University of Pavia, via Bassi 6, 27100 Pavia, Italy
[20]Institute of Physics, Polish Academy of Sciences, Aleja Lotnikow 32/46, PL-02668 Warsaw, Poland
[21]INFN Genova, via Dodecaneso 33, 16146 Genova, Italy

Abstract. Low-temperature antihydrogen atoms are an effective tool to probe the validity of the fundamental laws of Physics, for example the Weak Equivalence Principle (WEP) for antimatter, and -generally speaking- it is obvious that colder atoms will increase the level of precision.

After the first production of cold antihydrogen in 2002 [1], experimental efforts have substantially progressed, with really competitive results already reached by adapting to cold antiatoms some well-known techniques previously developed for ordinary atoms. Unfortunately, the number of antihydrogen atoms that can be produced in dedicated experiments is many orders of magnitude smaller than of hydrogen atoms, so the development of novel techniques to enhance the production of antihydrogen with well defined (and possibly controlled) conditions is essential to improve the sensitivity.

We present here some experimental results achieved by the AEgIS Collaboration, based at the CERN AD (Antiproton Decelerator) on the production of antihydrogen in a pulsed mode where the production time of 90% of atoms is known with an uncertainty of $\sim$ 250 ns [2]. The pulsed antihydrogen source is generated by the charge-exchange reaction between Rydberg positronium (Ps^*) and an antiproton ($\bar{p}$): $\bar{p} + Ps^* \rightarrow \bar{H}^* + e^-$, where Ps^* is produced via the implantation of a pulsed positron beam into a mesoporous silica target, and excited by two consecutive laser pulses, and antiprotons are trapped, cooled and manipulated in Penning-Malmberg traps.

The pulsed production (which is a major milestone for AEgIS) makes it possible to select the antihydrogen axial temperature and opens the door for the tuning of the antihydrogen Rydberg states, their de-excitation by pulsed lasers and the manipulation through electric field gradients.

In this paper, we present the results achieved by AEgIS in 2018, just before the Long Shutdown 2 (LS2), as well as some of the ongoing improvements to the system, aimed at exploiting the lower energy antiproton beam from ELENA [3].

1 Introduction

Experimental evidence has demonstrated that things fall in the Earth's gravitational field, at the same place, with the same acceleration regardless of their mass and composition. In fact, already in the seventeenth century Newton [4] realised that inertial and gravitational masses must be equal, establishing what is now called the Weak Equivalence Principle (WEP).

More than two centuries later, the Einstein Equivalence Principle (EEP), a cornerstone of the General Relativity [5], was proposed by Einstein in 1916 as an extension of the WEP. Einstein stipulated the WEP's validity as a prerequisite in his formulation of the equivalence principle.

Today, the WEP has undergone considerable experimental testing, and very strict constraints on its potential violation with ordinary matter have been established ($< 10^{-15}$), see the review [6] as well as the most recent results [7]. Moreover, the WEP should hold for antimatter, according to various theoretical and experimental considerations although these arguments are indirect and rely on certain theoretical presumptions. Conversely, the majority of attempts at a quantum theory of gravity predict novel interactions that could violate the WEP for antimatter (see e.g. [8]).

The goal of the AEgIS (Antimatter Experiment: gravity, Spectroscopy, Interferometry) experiment is to perform a direct test of the WEP on antimatter by measuring the acceleration of a cold antihydrogen beam in Earth's gravitational field [9], and its development is based on the idea of determining the vertical displacement due to gravity of an antihydrogen beam passing through a moiré deflectometer coupled to a position sensitive detector, akin to the one presented in [10]. The next section will provide an overview of the AEgIS experiment and procedure, which finds its foundations in a resonant charge-exchange process ([11, 12]).

2 Experimental apparatus and method

Differently from other antihydrogen experiments also based at the CERN AD (ATHENA [1], ATRAP [13], ALPHA [14] and ASACUSA [15]), that require the adjacent confinement of clouds of oppositely charged cold particles (antiprotons and positrons), our experiment necessitate to set up a sample of trapped antiprotons as well as a pulsed source of Ps^*. In the past, another experiment exploited the resonant charge exchange reaction between antiprotons and Ps^*, mediated by laser-excited cesium atoms (ATRAP [16]), but -as the experiments mentioned before- it led to a continuous antihydrogen production, while AEgIS method has the advantage to produce antihydrogen in a very short ($\sim$ 250 ns) temporal window.

Since the charge exchange cross section depends only on the relative velocity v_r between $\bar{p}$ and Ps^*, absolute velocities are in principle irrelevant, but in our conditions ($T_{\bar{p}} \simeq 400$ K, $v_{Ps^*,avg} \simeq 10^5$ m/s [17]) we can say that the relative velocity is mainly given by the Ps^* velocity itself. As a consequence, $\bar{p}$ cooling would have no effect on the production rate for us, although we need that antiprotons are cold enough to have the full efficiency in $\bar{H}$ detection (since the velocity of the resulting $\bar{H}$ is dominated by that of the $\bar{p}$, and the detector efficiency is reduced right after Ps^* is produced). On the other hand, it is clear that also cold Ps^* would be beneficial, because the reaction cross section drops suddenly for v_r higher than the e^+ velocity in the classical Ps orbit [18, 19]: in our case, $n_{Ps} \simeq 17$ and the cross section is negligible for $v_r \gtrsim 1.3 \cdot 10^5$ m/s.

Figure 1a shows the main elements of the AEgIS apparatus where $\bar{p}$ and Ps^* are prepared. All the charged particles, namely e^+, $\bar{p}$ and e^- (used to cool antiprotons by Coulomb collisions), are confined and manipulated inside Malmberg-Penning traps [20, 21] built with a sequence of cylindrical electrodes of different lengths, disposed in Ultra High Vacuum at cryogenic temperatures, aligned with the magnetic field produced by superconducting solenoids. Each electrode has a slice replaced by a metallic grid to get Ps^* into the trap.

Summarising, we catch and stack multiple antiprotons bunches (typically 8), delivered by the AD, in a trap region called "5 T trap" and we cool them by collisions with electrons which, in turn, loose their radial energy in the high magnetic field (precisely 4.46 T). The mixed $\bar{p}/e^-$ non-neutral plasma is then radially compressed [22–24] and then antiprotons are ballistically transferred along the expanding magnetic field lines into the region called "1 T trap" because of its lower magnetic field, where further cooling with electrons is performed.

At the end of this preparation, that usually takes $\sim$ 15 minutes, we obtain up to 10^6 $\bar{p}$ trapped with about 10^6 e^- in a quasi-harmonic potential ready for possible $\bar{H}$ formation. We infer the radial shape of the plasma with an imaging system made of a downstream on-axis Micro Channel Plate (MCP) coupled to a phosphor screen read out by a CMOS camera [22], while the number of e^- is measured by means of signals collected on a Faraday cup and the number of $\bar{p}$ is inferred from signals in external scintillators. The size of the $\bar{p}$ plasma is typically around 1 mm. We keep $\bar{p}$ plasma confined for some thousands of seconds with some expansion and negligible antiproton losses.

While antiprotons are prepared in this way, e^+ are stacked in a Surko-type accumulator based on a $\sim$ 1 GBq ^{22}Na source. Once the antiprotons are ready, a bunch of typically $2 \cdot 10^6$ positrons (with a temporal width shorter than $\sim$10 ns) is released every $\sim$ 100 s, is accelerated in flight to 4.6 keV and is magnetically transported along the B-field. This bunch is eventually smashed into the $e^+ - Ps$ converter, a cryogenic nanoporous target [25] which is situated close to the 1 T $\bar{p}$ trap (see Figure 1b).

The formed ortho-positronium (the para-positronium being too short lived in this regard) is emitted by the converter with kinetic energy $\sim$3 eV [26] and it is slowed down by collisions with the nanochannel walls until it is emitted in vacuum. After leaving the converter, it is ex-

*e-mail: zurlo@cern.ch

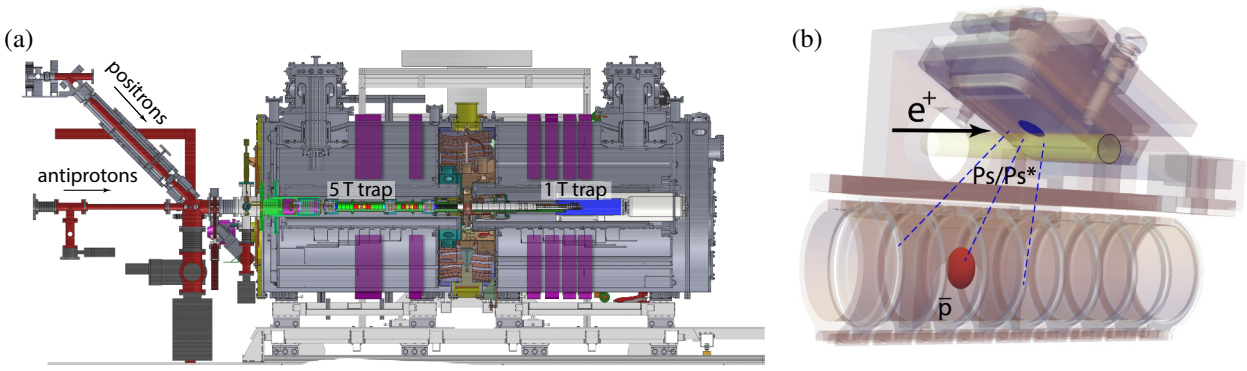

Figure 1. Drawing of the experimental apparatus. In violet, the external scintillator detector array, mentioned in the text (b): Enlargement of the $\bar{H}$ production region, located in the centre of the 1 T trap. In red: the antiproton plasma, inside a classical multi-ring trap hosting a mesh in the upper part. In blue: the nanoporous silica converter region where positrons impinge producing *Ps*, which is subsequently excited by two pulsed laser beams (sketched in yellow).

cited to a Rydberg state with principal quantum number $n \simeq 17$ through two subsequent laser pulses [27, 28] (the first from $n = 0$ to $n = 3$; the second to the targeted n). The time when the first laser is fired is the reference time for our pulsed scheme: this time is known with few-ns-accuracy.

Given the typical time spread of the target-hitting e^+ pulse of < 10 ns, and the *Ps* cooling time in the converter of the order of ten ns, the major uncertainty on the $\bar{H}$ production time is due to the Ps^* velocity spread that affects the time of flight needed to reach the $\bar{p}$ cloud. With the *Ps* velocity distribution measured in dedicated experiment [17], this time is a few hundreds of ns.

3 Results

First, we should recall that any antihydrogen produced, differently from trapped antiprotons, would be unconfined by the Penning trap fields and would eventually annihilate on the trap walls after a short drift time. The annihilation products from the antiproton annihilation (manly charged pions) can be then detected by the external scintillator detector array. In practice, there are also small, continuous losses of antiprotons in the Penning trap, due to collisions on the residual gas and to trap imperfections that make the antiproton plasma slowly expand and the peripherals antiprotons collide with the trap wall. These "lost antiprotons" produce a signal that in our detectors is totally similar to the one generated by antihydrogen: this is the reason why it so important to estimate accurately this "background signal", as we will explain later.

The detection of the events discussed here was performed with the so-called "External scintillator detector array" (see Figure 1a), situated outside the superconducting solenoids. To be precise, it consisted of 12 plastic (EJ200) arc-shaped scintillating slabs, 1 cm thick and 10 or 20 cm wide, coupled to two photomultipliers (PMTs), one at each end. Each scintillator was designed to cover a 120° angle centred around the vertical plane containing the solenoid axis and was situated either above or below the main cryostat.

Differently from "standard" data acquisition, relying on the signal produced by CAEN N413, LeCroy 623A and LeCroy 622 discriminators and essentially taken via the coincidence between the two photomultipliers connected to the same slab (that was not sensitive enough to effectively count the few antihydrogen annihilations over the antiproton annihilations/cosmic rays/environmental background), we developed a different, more accurate approach for the record and the analysis of the scintillator data in a convenient time window around the time of the positron injection, where antihydrogen production had to be investigated. In fact, through CAEN V1720 modules we recorded the full digitised photomultiplier signals with a sampling frequency of 250 MHz in a time window that can be as wide as a ~5 ms (actually, 1/8 of this duration was sufficient in our case). These signals were subsequently exploited offline only after averaging the signal between the two photomultipliers reading the same scintillating slab, to compensate for light attenuation inside each slab. After an accurate calibration of each PMT, the signal amplitude could be considered an excellent proxy for the energy deposit inside the scintillator by the charged particles passing through it, as reported in [29], so different efficiencies are expected for antiproton/antihydrogen annihilations, *Ps* annihilations and cosmic/environmental background, depending on the energy loss distribution and on the selected threshold. The mentioned digital acquisition of the full PMT signals, together with an accurate threshold optimisation, guided by a detailed Monte Carlo simulation of the full system based on Geant4 (using cosmic muons energy loss for reference, see [30–32] for further details on the cosmic muon generator), allowed us to improve the signal over background ratio for $\bar{p}$ annihilation excess, which in turn is a clear signature for $\bar{H}$ annihilation.

To demonstrate antihydrogen production, we have performed experiments in 3 different conditions, always with

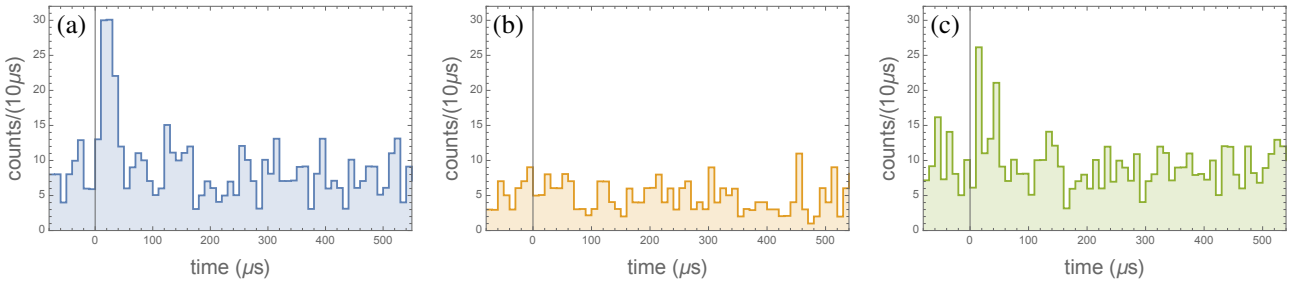

Figure 2. Time distribution scintillator pulses. (a) Experiment with $\bar{p}$, e^+ and laser (2206 cycles, $1.08 \times 10^9\,\bar{p}$). (b) Experiment with $\bar{p}$, e^+ and without laser (1211 cycles, $6.08 \times 10^8\,\bar{p}$). (c) Experiment with $\bar{p}$, laser and without e^+ (3498 cycles, $1.58 \times 10^9\,\bar{p}$). Notice that the overall number of cycles is different for each typology of data; in order to make a direct comparison, histogram renormalization should be applied.

antiprotons stored in the Penning-Malmberg trap. First, we took sequences of runs with e^+ injection, subsequent *Ps* production and laser excitation in nominal conditions (Figure 2a): these are all the ingredients needed to form $\bar{H}$. Then we took cycles without extracting e^+ from the accumulator (Figure 2b) and finally cycles without firing the laser (Figure 2c). In the last two kind of runs, $\bar{H}$ formation is inhibited by the absence of some of the essential ingredients to produce it.

The full signal was acquired for a 650 μs-long time window, starting 50 μs before the laser shot ($t = 0$), in order to have a convenient control time window. Unfortunately, the first 1 μs after the positron injection the detector was blind because it needed time to recover from the saturation experienced right after the positron bunch injection, which produced a large number of simultaneous e^+ annihilations.

From Figure 2a we can infer that there is a signal just after $t = 0$ when we had antiprotons, e^+ injection and laser. This signal occurs between t=1 μs and t=26 μs, consistently with the mentioned saturation of the detector in the first μs. On the other hand, without firing the laser (Figure 2b), the signal was reduced to the temporally-uniform background, due to cosmic rays and $\bar{p}$ losses, as expected. It must be also mentioned (see Figure 2c) that some (but fewer) excess events are present also in the runs with $\bar{p}$ and the laser but without e^+ injection, that we interpret as a possible background of $\bar{p}$ annihilations due to the laser-induced outgassing from the cryogenic surfaces. Summarising, we observed 79 events in the signal region while we expect to detect 33.4 ± 4.6 events under the hypothesis of absence of $\bar{H}$ formation (see [2] for a more detailed discussion of the statistical significance).

4 Improvements after 2018

During and after the CERN LS2, an appreciable number of improvements has been implemented on the system to enhance the overall performance (and antihydrogen yield in particular).

First, the focus was on positrons and positronium. The experiment design has been revised: since the old setup (Figure 1b) was based on a *Ps*-producing converter situated on top of the $\bar{p}$ trap, the motional Stark effect prevented *Ps* atoms moving perpendicularly to the magnetic field from being excited to higher Rydberg state [17]. During the LS2, it was modified into a fully collinear setup, where the converter is aligned with axis of the $\bar{p}$ trap whose electrodes in turn can have larger size since their radius is not limited by the distance to the converter. In principle, this should lead approximately to a 4-fold improvement in antihydrogen yield.

At the same time, the preparation of the e^+-*Ps* converter was improved [33] ($\sim$ 3-fold improvement in antihydrogen yield) and new diagnostic tools were developed [34, 35].

On the antiproton side, the commissioning of the ELENA ring allows now the capture of a much larger number of antiprotons, assuming equal catching potentials and optimal degrader foil thicknesses (besides the fact that in the new system the high voltage for catching antiprotons has been slightly increased with respect to 2018). In fact, the AD delivered a bunch of $\sim 3 \cdot 10^7\,\bar{p}$ with 5.3 MeV kinetic energy (100 MeV/c momentum) every 100 s that where reduced by a factor of $\sim$ 100 after catching, while ELENA releases $\sim 6 \cdot 10^6\,\bar{p}$ with 100 keV kinetic energy (13.7 MeV/c momentum) with comparable repetition rate, but with much higher catching efficiency for the related experiments (first measurements suggest that for AEgIS it could be better than $\sim$ 60%). In principle, this should reflect a $\sim$ 4-fold improvement in antihydrogen yield.

Other upgrades concern the laser system (in particular a new alexandrite laser system for a more efficient *Ps* excitation), the electronics for the nanosecond control system to set the voltages on the trap electrodes (which has been moved to the Sinara hardware family driven by the ARTIQ library system, which in turn is based on Python) as well as the overall software (where a new distributed, modular control system arranged in micro-services and programmed in Labview™ has been implemented to run the experiment). The new laser system is meant essentially to improve the long term stability of the cavity and, because of the wider laser bandwidth, also the antihydrogen yield should benefit. The control system upgrades were devel-

oped mainly for an improvement in ease of operation of the experiment.

In principle, if everything works as per design, the antihydrogen yield should increased by one or two orders of magnitude.

5 Conclusions

We have presented the first AEgIS results about $\bar{H}$ pulsed production, based the 'resonant" charge exchange reaction between $\bar{p}$ and laser-excited Ps^*. Till now, this is the $\bar{H}$ production scheme with the most precise time tagging ever achieved.

Although we have confirmed that the the $\bar{H}$ signal is not consistent with the background, the production rate is still extremely low: on average, less than 0.1 $\bar{H}$ for a typical cycle operated in 2018. In fact, substantial upgrades are being implemented to improve the overall experiment.

References

[1] M. Amoretti et al., *Production and detection of cold antihydrogen atoms*, Nature 419, 456 (2002).

[2] C. Amsler et al., *Pulsed production of antihydrogen*, Commun. Phys. 4, 19 (2021). DOI:10.1038/s42005-020-00494-z

[3] W. Bartmann et al. on behalf of the ELENA and AD teams, *The ELENA facility*, Phil. Trans. R. Soc. A 376: 20170266 (2018). http://dx.doi.org/10.1098/rsta.2017.0266

[4] I. Newton, *Philosophiae Naturalis Principia Mathematica*, Londini: Jussu Societatis Regae ac Typis Josephi Streater: Prostant Venales apud plures Bibliopolas (1687).

[5] A. Einstein, *Die Grundlage der allgemeinen Relativitätstheorie*, Annalen der Physik, Vol. 49, p.769 (1916).

[6] C. M. Will, *The Confrontation between General Relativity and Experiment*, Living Reviews in Relativity, Vol. 17, 4 (2014).

[7] P. Touboul et al., *MICROSCOPE Mission: Final Results of the Test of the Equivalence Principle*, Phys. Rev. Lett. 129, 121102 (2022).

[8] V. A. Kostelecký and J. D. Tasson, *Matter-gravity couplings and Lorentz violation*, Phys. Rev. D 83, 016013 (2011).

[9] M. Doser et al. (AEgIS Collaboration), *Exploring the WEP with a pulsed beam of cold anihydrogen*. Class. Quantum Grav. Vol. 29, p. 213 184009 (2012).

[10] S. Aghion et al. (AEgIS Collaboration), *A moiré deflectometer for antimatter*, Nat. Commun., Vol 5, p.4538, (2014). DOI: http://dx.doi.org/10.1038/ncomms5538

[11] B. I. Deutch, A. S. Jensen, A. Miranda and G. C. Oades, Proceedings of The First Workshop on Antimatter Physics at Low Energy, 371, FNAL (1986).

[12] M. Charlton, *Antihydrogen production in collisions of antiprotons with excited states of positronium*, Physics Letters A, Vol. 143 (3) 143 (1990).

[13] G. Gabrielse et al., *Driven production of cold antihydrogen and the first measured distribution of antihydrogen states*. Phys. Rev. Lett. 89, 213401 (2002). DOI:10.1103/PhysRevLett.89.213401

[14] G. B. Andresen et al. *Trapped antihydrogen*, Nature Vol. 468, p. 673 (2010).

[15] N. Kuroda et al. *A source of antihydrogen for in-flight hyperfine spectroscopy*, Nat. Commun., Vol. 5, p.3089 (2014).

[16] C. H. Storry et al., *First Laser-Controlled Antihydrogen Production* , Phys. Rev. Lett. 93, 263401 (2004).

[17] M. Antonello et al., *Rydberg-positronium velocity and self-ionization studies in a 1T magnetic field and cryogenic environment*, Phys. Rev. A 102, 013101 (2020).

[18] D. Krasnicky, R. Caravita, C. Canali and G.Testera, *Cross section for Rydberg antihydrogen production via charge exchange between Rydberg positroniums and antiprotons in a magnetic field*, Phys. Rev. A 94, 022714(14) (2016).

[19] D. Krasnicky, G. Testera and N. Zurlo, *Comparison of classical and quantum models of anti-hydrogen formation through charge exchange*, J. Phys. B: At. Mol. Opt. Phys. 52, 115202 (2019).

[20] F. G. Major, V. N. Gheorghe and G. Werth, *Charged Particle Traps Springer Series on Atomic, Optical, and Plasma Physics*, Springer-Verlag Berlin Heidelberg (2005).

[21] D. H. E. Dubin and T. M. O'Neil, *Trapped nonneutral plasmas, liquids, and crystals (the thermal equilibrium states)*. Rev. Mod. Phys. 71, 87-172 (1999).

[22] S. Aghion et al., (AEgIS Collaboration), *Compression of a mixed antiproton and electron non-neutral plasma to high densities*. Eur. Phys. J. D 72, 76-86 (2018).

[23] G. B. Andresen et al., (ALPHA Collaboration), *Compression of antiproton clouds for antihydrogen trapping*. Phys. Rev. Lett. 100, 203401 (2008).

[24] N. Kuroda et al., *Radial compression of an antiproton cloud for production of intense antiproton beams*. Phys. Rev. Lett. 100, 203402 (2008).

[25] S. Mariazzi, P. Bettotti and R. S. Brusa, *Positronium Cooling and Emission in Vacuum from Nanochannels at Cryogenic Temperature*, Phys. Rev. Lett. Vol. 104 p. 243401 (2010).

[26] Y. Nagashima et al., *Origin of positronium emitted from SiO_2*, Phys. Rev. B 58, 12676-12679 (1998).

[27] S. Aghion et al. (AEgIS Collaboration), *Laser excitation of the n = 3 level of positronium for antihydrogen production*, Phys. Rev. A 94, 012507 (2016).

[28] M. Antonello et al. (AEgIS Collaboration), *Rydberg-positronium velocity and self-ionization studies in 1T magnetic field and cryogenic environment*, Phys. Rev. A 102, 013101 (2020).

[29] N. Zurlo et al. (AEgIS Collaboration), *Calibration and equalisation of plastic scintillator detectors for antiproton annihilation identification over positron/positronium background*, Acta Physica

Polonica B, Vol. 51, No 1, p. 213 (2020).

[30] D. Pagano, G. Bonomi, A. Donzella, A. Zenoni, G. Zumerle and N. Zurlo, *EcoMug: An Efficient COsmic MUon Generator for cosmic-ray muon applications*, Nucl. Instrum. Meth. Phys. Res. A 1014, 165732 (2021). DOI: https://doi.org/10.1016/j.nima.2021.165732

[31] G. Bonomi, A. Donzella, D. Pagano, A. Zenoni, G. Zumerle and N. Zurlo, *A Monte Carlo Muon Generator for Cosmic-Ray Muon Applications* Journal of Advanced Instrumentation in Science, Vol. 2022 (2022). DOI: https://doi.org/10.31526/jais.2022.290.

[32] N. Zurlo, G. Bonomi, A. Donzella, D. Pagano, A. Zenoni and G. Zumerle, *A new Monte Carlo muon generator for cosmic-ray muon applications*, Proceedings of Computational Tools for High Energy Physics and Cosmology — PoS(CompTools2021), Vol.409, p.019 (2022). DOI: https://doi.org/10.22323/1.409.0019

[33] S. Mariazzi et al. (AEgIS Collaboration), *High-yield thermalized positronium at room temperature emitted by morphologically tuned nanochanneled silicon targets* J. Phys. B: At. Mol. Opt. Phys. 54 085004 (2021).

[34] C. Amsler et al. (AEgIS Collaboration), *A ∼100 μm-resolution position-sensitive detector for slow positronium* Nucl. Instrum. Meth. Phys. Res. B 457, 44-48 (2019).

[35] L. Glöggler et al. (AEgIS Collaboration), *High-resolution MCP-TimePix3 imaging/timing detector for antimatter physics* Meas. Sci. Technol. 33 115105 (2022).